DOT/FAA/AM-21/4
Office of Aerospace Medicine
Washington, DC 20591

CARI Documentation: Particle Spectra

Kyle Copeland

Civil Aerospace Medical Institute
Federal Aviation Administration
Oklahoma City, OK 73125Location/Address

March 2021

Final Report

NOTICE

Technical Report Documentation Page

1. Report No.	2. Government Accession No.	3. Recipient's Catalog No.
DOT/FAA/AM-21/4		

4. Title and Subtitle	5. Report Date
CARI-7 DOCUMENTATION: PARTICLE SPECTRA	March 2021
	6. Performing Organization Code
7. Author(s) Copeland, K.	8. Performing Organization Report No.
9. Performing Organization Name and Address Civil Aerospace Medical Institute FAA	10. Work Unit No. (TRAIS)
	11. Contract or Grant No.
12. Sponsoring Agency name and Address Office of Aerospace Medicine Federal Aviation Administration 800 Independence Ave., S.W. Washington, DC 20591	13. Type of Report and Period Covered
	14. Sponsoring Agency Code

15. Supplemental Notes

16. Abstract

This report presents the solar and galactic cosmic radiation models, solar modulation algorithms, and data used by CARI (i.e., the Civil Aviation Research Institute—the previous name of the Civil Aerospace Medical Institute, or CAMI) software version 7 (CARI-7) and -7A. CARI software for calculating doses of ionizing radiation in the atmosphere from cosmic radiation has been in development at CAMI since the late 1980s. The accurate calculation of galactic and solar cosmic radiation dose rates and other related quantities in near-Earth space and within Earth's atmosphere requires knowledge of the incoming energetic ions present in galactic and solar cosmic radiation. Like previous versions of CARI software, CARI-7 uses the heliocentric model of solar modulation of galactic cosmic radiation, but unlike prior versions, CARI-7 uses the local interstellar spectrum described in the International Standards Organization standard TS15930:2004. CARI-7A offers additional galactic and solar cosmic radiation spectra, and allows use of a user-defined spectrum.

17. Key Words	18. Distribution Statement
Ionizing Radiation, Cosmic Radiation, Space Weather, Cosmic Radiation Models, CARI-7, CARI-7A, Solar Modulation.	Document is available to the public through the Internet: http://www.faa.gov/go/oamtechreports/

19. Security Classif. (of this report)	20. Security Classif. (of this page)	21. No. of Pages	22. Price
Unclassified	Unclassified	21	

Form DOT F 1700.7 (8-72) Reproduction of completed page authorized

ACKNOWLEDGMENTS

The author gives special thanks to Keran O'Brien for his work on heliocentric potentials calculated for CARI-6 and earlier versions of CARI; Patrick O'Neill for providing and allowing the inclusion of the 2011 and 2014 versions of the Badhwar and O'Neill GCR models and his comments on how to use them appropriately; World Data Center for Cosmic Rays, Ibaraki, Japan for neutron monitor data; the Polar Geophysical Institute and Dr. Balabin, Apatity, Russia, for Apatity neutron monitor data; the NOAA Space Weather Prediction Center for access to solar particle event data; and David Nelms, Webmaster of the Civil Aerospace Medical Institute (CAMI), for help in maintaining the CARI program-related webpages. This work is in partial fulfillment of Project 2017-AAM-631-NUM-10114 sponsored by the Federal Aviation Administration's Office of Aerospace Medicine.

CONTENTS

EXECUTIVE SUMMARY

This report presents the solar and galactic cosmic radiation models, solar modulation algorithms, and data used by CARI (i.e., the Civil Aviation Research Institute—the previous name of the Civil Aerospace Medical Institute, or CAMI) software version 7 (CARI-7) and -7A. CARI software for calculating doses of ionizing radiation in the atmosphere from cosmic radiation has been in development at CAMI since the late 1980s. The accurate calculation of galactic and solar cosmic radiation dose rates and other related quantities in near-Earth space and within Earth's atmosphere requires knowledge of the incoming energetic ions present in galactic and solar cosmic radiation. Like previous versions of CARI software, CARI-7 uses the heliocentric potential model of solar modulation of galactic cosmic radiation, but unlike prior versions, CARI-7 uses the local interstellar spectrum described in the International Standards Organization standard TS15930:2004. CARI-7A offers additional galactic and solar cosmic radiation spectra, and allows use of a user-defined spectrum.

CARI Documentation: Particle Spectra

BACKGROUND

Early Cosmic Ray Research

The first experimental results hinting at the phenomenon known as *cosmic radiation* were from a German Jesuit monk and physicist, Theodore Wulf, who had developed a special electrometer to study ionizing radiation emanating from the ground (Hörandel, 2013). In 1909 and 1910, he carried out measurements with his instrument at diverse locations, including the top and bottom of the Eiffel tower, and was surprised when his measurements atop the Eiffel Tower (a height of 300 meters) were not reduced by as much as he expected based on the distance above the ground. Victor Hess, studying at the Radium Institute in Vienna, decided to take the experiment a step further, making a series of balloon flights from 1911 to 1913 (Perricone, 2001). Expecting the that radiation from the ground would dissipate at an altitude of 500 m, he was surprised to find that while it decreased at first, in keeping with his prediction, it then started rapidly increasing as he continued to ascend. He is conclusion was that "a radiation of very high penetrating power enters our atmosphere from above." Also, because ionization did not decrease on his flight during a solar eclipse[1] (April 12, 1912), he was convinced that the Sun could not be this radiation's primary source. In 1936 Hess was awarded Nobel Prize in physics for his work (Nobel Foundation, 1965).

The cosmic radiation that originates from outside our solar system is called *galactic cosmic radiation* (GCR). The principal source of this radiation in our part of the galaxy is stellar material and surrounding interstellar gas, accelerated as a result of stellar explosions called *supernovae*. Stellar winds of stars much more massive than the Sun are also thought to be an important source. However, the rarest, highest-energy GCR particles are believed to come from nearby galaxies with central black holes ejecting jets of plasma (a gas with a portion of its components ionized) into intergalactic space (Pierre Auger Collaboration, 2007). GCR particles usually are fully ionized. While nuclei of every naturally occurring element are present, most are protons (hydrogen nuclei) or alpha particles (helium nuclei). There are also some electrons and very energetic photons. The charged particles typically spend millions of years traveling convoluted paths (warped by the galactic magnetic field) through the space between their sources and our solar system. Until the building of powerful particle accelerators, cosmic radiation research was the primary source of data for the science of high-energy nuclear physics.

Solar Wind

The number of GCR particles that enter the atmosphere varies inversely with the rise and decline in solar activity, resulting in variations in radiation dose rates in the atmosphere. The variations are caused by magnetic fields carried by the *solar wind*. The source of the solar wind is particles from a layer of the Sun's atmosphere called the *corona* (Appendix A). The corona's temperature is so high that some of its particles are always escaping the Sun's gravity. Compared to cosmic rays, these are very low energy

---

[1] While his conclusion was correct, his reasoning was not. He reasoned that during a solar eclipse, the Moon passes between the Earth and the Sun, blocking radiation travelling along the Sun-Earth line of sight. It was not known at the time that energetic solar ions follow a curved path because of the interplanetary magnetic field.

particles but remain much too low in energy to directly cause an increase in ionizing radiation levels at aircraft flight altitudes. The particles are charged and carry irregularities in the Sun's magnetic field through interplanetary space. The irregularities in these magnetic fields scatter low-energy GCR particles that might otherwise enter the Earth's atmosphere (Wilson, 1976). When solar activity is high, the solar wind carries more irregularities, resulting in more scattering of low-energy GCR particles and a corresponding decrease in dose rates.

There are almost 300 years of sunspot[2] records, which indicate changing solar conditions (Sunspot Index and Long-term Solar Observations [SILSO], n.d.). These data indicate solar activity has varied in approximately 11.1-year cycles, which we now know correspond to solar magnetic pole reversals (Smart and Shea, 1997). Sunspot numbers firmly anti-correlate with more modern GCR measures, such as secondary neutron flux reaching the Earth's surface and satellite-based measurements of cosmic radiation particle flux (McDonald et al., 2010). These more modern observations of solar modulation of GCR led to the development of parameters such as Ehmert potential, heliocentric potential, and solar modulation potential as indicators of the influence of solar activity on GCR at Earth and throughout the solar system (Ehmert, 1959; O'Brien, 1979; O'Neill, 2010). Figure 1 shows monthly International Sunspot Number (ISSN) and CARI (i.e., the Civil Aviation Research Institute—the previous name of the Civil Aerospace Medical Institute, or CAMI) software version 6 (CARI-6) heliocentric potential from 1976 through 2017.

Figure 1

Monthly Averaged International Sunspot Numbers and CARI-6 heliocentric potentials: January 1976-January 2018

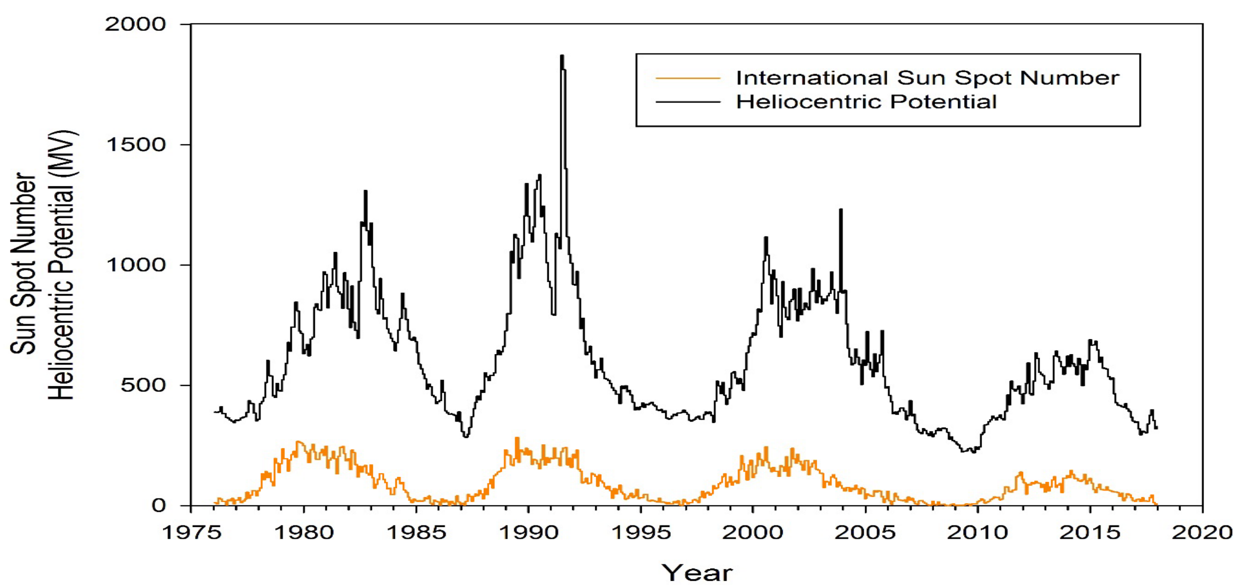

Note. From Sunspot Index and Long-term Solar Observations (n.d.) and the Federal Aviation Administration (2017).

---

[2] A sunspot is an area on the photosphere that is seen as a dark spot in contrast with its surroundings. Sunspots appear dark because the area is cooler than the surrounding photosphere. Sunspots occur where areas of the Sun's magnetic field loop up from the surface of the Sun and disrupt convection of hot gases from below.

Solar Particle Events

Magnetic disturbances near and above the Sun's surface called *solar flares* and *coronal mass ejections (CMEs)* result in explosive emissions of huge amounts of solar matter consisting mostly of ionized, relatively low-energy particles. Through a process called *shock acceleration*, these low-energy particles can accelerate ions higher in the solar atmosphere and interplanetary space to speeds similar to those of GCR. These accelerated particles are referred to as *solar cosmic radiation* (SCR) and occasionally significantly increase the flux of very energetic ions in Earth's atmosphere. Such an increase at Earth is referred to by various terms: *solar-particle event*, *solar-proton event* (SPE), *solar energetic-particle event*, and *solar cosmic-ray event* (all referred to herein as SPE). During an SPE, the SCR that enters the Earth's atmosphere interacts with air atoms in the same way as GCR. With regard to radiation exposure of aircrews, the most important SCR primary particles are protons, while SCR alpha particles can contribute several percent of the effective dose at aviation altitudes.

Although they can occur at any time during the solar cycle (Figure 2), SPEs occur more often during the active period of the solar cycle (National Oceanic and Atmospheric Administration [NOAA], n.d.-b; Smart and Shea, 1997). The earliest-arriving particles come from the direction of the Sun, but soon solar particles are coming from all directions because of the bending effects on the particle paths caused by both interplanetary and Earth's magnetic fields. One-half to a few hours after the start of an event, radiation levels in the atmosphere on the dark and light sides of the Earth come close to being the same (Foelsche et al., 1974).

Figure 2

Occurrence of Solar Proton Events During the Last Few Solar Cycles as Represented by Peak Flux on the S-Scale *With ISSN and Neutron Monitor Count Rates*

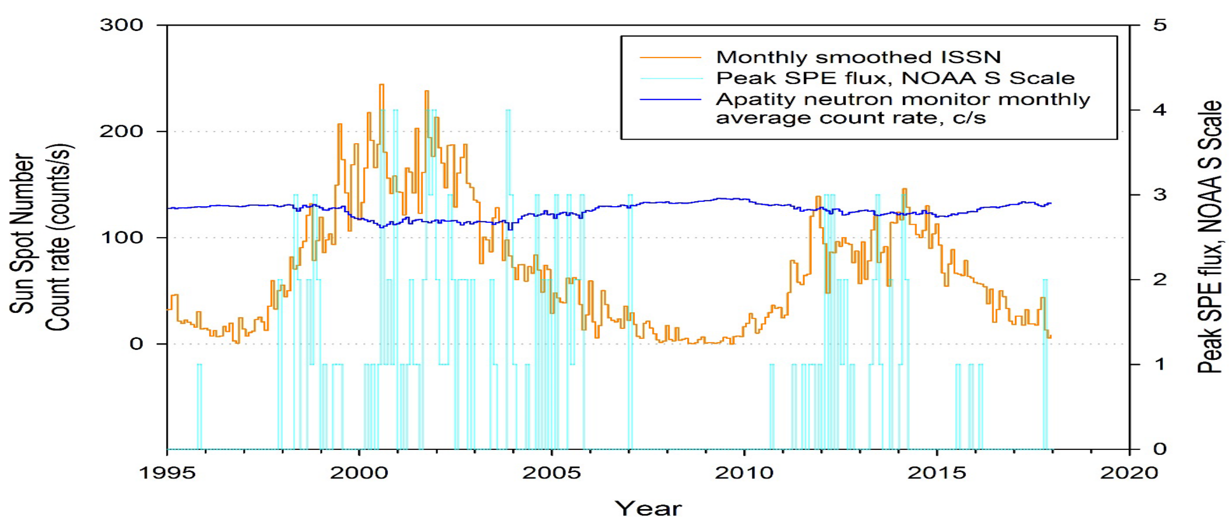

Note. ISSN = International Sunspot Number; SPE = Solar-proton event; NOAA = National Oceanic and Atmospheric Administration.

Data are from NOAA (n.d.-a), SILSO (n.d.), NOAA (n.d.-b), and the Polar Geophysical Institute (n.d.).

Decades of study indicates that while there are many common features, each SPE is unique, and currently, their early evolution is unpredictable. Arrival directions for particles of a given energy are dependent upon several constantly changing factors, such as the interaction between the Earth's magnetic field and the interplanetary magnetic field. When compared with the GCR doses rates for the same altitude, the increase in dose rates is usually small for aircrews, but it is unknown how high the radiation levels will reach even after the event has begun. On rare occasions, a solar-proton event can result in a substantial short-term increase in ionizing radiation at commercial flight altitudes (Copeland et al., 2008; Copeland and Atwell, 2019).

Forbush Decrease

Most SPEs do not significantly increase radiation dose rates deep in Earth's atmosphere. They can still affect dose rates; however, deflecting GCR in a manner similar to the normal solar wind. This kind of decrease in GCR is referred to as a *Forbush decrease* (Forbush, 1938; Smart and Shea, 1997; Oh et al., 2008) and can occur during (typically at the time of the arrival of the CME shock front) or in the absence of an SPE at Earth. The strength of the decrease is controlled by the size of the CME, the complexity and strength of its embedded magnetic fields, and its movement through the solar system.

MODEL DESCRIPTIONS

Galactic Cosmic Radiation Outside of the Heliosphere

CARI-7A (Copeland 2017) offers four internal options regarding the primary GCR spectrum model, based upon three different assumed particle spectra in local interstellar space (*local interstellar spectrum* [LIS]). CARI-7 and -7A use elements hydrogen ($Z = 1$) to nickel ($Z = 28$) of the LIS from each model. While the agreement between models is generally good, there are some crucial differences evident at low energies and the various ions' spectral indices. For each of the models, the effect of Forbush decreases on primary GCR flux is handled independently of the GCR model chosen. In the next three sections, each model is described in more detail.

For both of the Badhwar and O'Neill models (O'Neill and Foster, 2013; O'Neill et al., 2015), the effects of transport through the heliosphere to Earth's magnetosphere on the GCR spectra (i.e., *solar modulation*) are handled within the respective GCR model, while for the International Standards Organization (ISO) model (ISO, 2004) solar modulation of the LIS can be handled as defined in the standard or by using heliocentric potentials.

International Standards Organization Model

This ISO GCR model is ISO TS15930:2004 spectrum (ISO, 2004). It establishes the model parameters and characteristics of variations in the 10^1 MeV to 10^5 MeV GCR particles (electrons, protons, and $Z = 2$ to 92 nuclei in the near-Earth space beyond the Earth's magnetosphere). Solar modulation is driven by sunspot number and date, used to find the solar magnetic field orientation. The model describes the variations of GCR fluxes due to variations in solar activity and the large-scale heliospheric magnetic field (the Sun's polar magnetic field) throughout 22-year cycles. Solar activity is characterized by 12-month running averages of Wolf sunspot numbers. These numbers are no longer published, so CARI now converts the data internally from published current data available from the Solar Influences Data Analysis Center (SIDC) team, World Data Center for the Sunspot Index, SILSO (n.d.), Monthly Report on the ISSN, online catalog of the sunspot index:

www.sidc.be/sunspot-data/1745-2013

For CARI-7A, the ISO model was coded directly from the ISO document describing the 2004 version of the standard, TS15930:2004. It is also known as the Moscow State University GCR spectrum and is a modern version of the Nymmik GCR spectrum (Nymmik et al., 1992). In 2013, the standard was reviewed and left unchanged.

Badhwar-O'Neill Models

The GCR model of Badhwar and O'Neill (1994, 1996) was initially developed to provide an accurate GCR energy spectrum that engineers could use in single-event effect rate prediction codes and radiation health physicists could use for astronaut exposures on deep space missions. The GCR model is designed for free space—beyond the Earth's magnetosphere. It uses the spherically symmetric Fokker-Planck equation that accounts for cosmic-ray propagation in the heliosphere due to diffusion, convection, and adiabatic deceleration. The boundary condition is the LIS for each GCR element at the outer edge of the heliosphere (assumed to be at 100 AU). The Fokker-Planck equation modulates the LIS to a given radius from the Sun—assuming steady-state heliosphere conditions.

The 2011 Badhwar-O'Neill Model

A 2009 study by Adams et al. (2009) showed that the 2004 version of the Badhwar-O'Neill model was less compatible with the older GCR data (1955–1997) compared to the Nymmik 1997 GCR model. In response to this critique, the older data was reexamined and combined with newer data (1997–2010). The result was a new model that agreed excellently with both the old and the new GCR data measurements (O'Neill, 2010; O'Neill and Foster, 2013). The least-square errors are within that expected for both the older and the newer instruments. This was considered a significant improvement to the overall accuracy of modeling the true GCR spectrum—based on 55 years of cosmic ray measurements—because spacecraft designers need the actual history of GCR fluxes because it is the best knowledge of actual worst-case conditions.

Like the ISO model, the BO11 model uses the correlation with the sunspot number to determine the level of solar modulation to a monthly level to allow users to take advantage of the predictive capability in the correlation. However, to enable increased accuracy (and finer time resolution), spacecraft data are used to calibrate the sunspot number for periods where they overlap—IMP-8 from 1974 to 1997 and ACE after 1997.

The stand-alone BO11 GCR model source code provided by Patrick O'Neill was modified slightly to allow incorporation into CARI-7A.

The Badhwar-O'Neill 2014 Model

The 2014 version of the Badhwar-O'Neill GCR model (BON14) continues the improvement of the original model (O'Neill et al., 2015). The technical paper describing the model includes the most recent improvements in parameter fits. A comprehensive measurement database is also used to show that BON14 is significantly improved over the previous version, BON11.

Unlike the BON11 and ISO models, Windows 64-bit and Scientific Linux executables, but not source code, were provided for the BON14 model. Incorporation into CARI-7A is, therefore, less complete. Non-Windows operating system (OS) users should contact model developers indicated in the report describing the model to obtain an executable for their particular OS.

Radiation Transport and Modulation of GCR in the Heliosphere

Forbush Decreases

To account for Forbush decreases and other minor variations from transient space weather in solar activity that affect GCR on the scale of an hour to a day (*t*), the approach used in CARI-7 and -7A is that proposed by Lantos (2005) and proceeds as described in Copeland (2014). GCR flux (ϕ) is modulated in direct proportion (1:1) to changes in neutron monitor count rate fluctuations (*N*) at a high-latitude, near-sea-level monitor:

$$\phi = \phi_{month}\left(\frac{N_t}{N_{month}}\right) \tag{1}$$

Hourly count rate changes relative to the monthly average from annual "longformat" data from the World Data Center for Cosmic Rays are used as the base data for the adjustments (Nagoya University, 2015). For periods of missing data and during solar proton events, no modulation is used (i.e., $N_t = N_{month}$). Hourly data from the Deep River neutron monitor data are used through September 1995. For more recent times, hourly data from the Apatity neutron monitor are used.

Solar Modulation in the ISO Model

In the ISO GCR model, the dynamics of the large-scale GCR modulation by the solar wind is characterized by the effective modulation potential of the heliosphere, $V(t,R)$, for particles of rigidity R at a given moment t, and is calculated as

$$V(t,R) = 0.37 + 3 \times 10^{-4} \times W(t - \Delta t(n,R,t))^{1.45}\ , \tag{2}$$

where $W(t)$ is the Wolf sunspot number for month t, R is the particle rigidity, n is the solar cycle number, and $\Delta t(n,R,t)$ is the lag (in months) of the GCR flux variations relative to solar activity variations and is given by,

$$\Delta t(n,R,t) = 0.5 \times [15 + 7.5 \times R^{-0.45}] + 0.5 \times [15 - 7.5 \times R^{-0.45}] \times \tau(W_{ave}), \tag{3}$$

with,

$$\tau(W_{ave}) = (-1)^n \times \left[\frac{W_{ave}(t-16) - W_{ave,n,min}}{W_{ave,n,max}}\right]^{0.2}, \tag{4}$$

where $W_{ave}(t)$ is the average Wolf number for the year around month *t*, $W_{ave,n,min}$ is the lowest yearly average Wolf number that borders solar cycle n, and $W_{ave,n,max}$ is the highest yearly average Wolf number that borders solar cycle n.

Solar Modulation in the Badhwar-O'Neill 2011 and 2014 Models

In the BON GCR models, the solar modulation potential, Φ (MV), is a parameter based on the GCR secondary neutron flux measurements reaching the Earth's surface (O'Neil, 2010; Mertens et al., 2013). This parameter is used with the Fokker-Plank equation to account for attenuation of the local interstellar spectrum within the heliosphere. A steady-state is assumed to be achieved by a dynamical balance between inward diffusion, adiabatic energy loss, and outward convection by a constant solar wind speed. The equation that embodies this assumption is

$$\frac{\partial(r^2 I(E))}{\partial r} - \frac{2r}{3}\frac{\partial}{\partial E}\left(E\,\Gamma(E)\,I(E)\right) - \frac{\partial}{\partial r}\left[\left(\frac{\kappa_0}{V_{sw}}\,\beta\,R\left[1+\left(\frac{r}{r_0}\right)^2\right]\Phi^{-1}\right) r^2 \frac{\partial I}{\partial r}\right] = 0. \quad (5)$$

In Eq. 5, I is the differential number density of the GCR gas with respect to E, the kinetic energy (in MeV) per nucleon, r is the radial distance from the Sun (in AU), and r_0 and κ_0 are constants equal to 4 AU and $1.6 \cdot 10^{21}$ $cm \cdot s^{-1}$, respectively. VSW denotes the constant solar wind speed (400 km.s-1), β is the ratio of the particle velocity to the speed of light, R is the particle magnetic rigidity (in MV), and $\Gamma(E)$ is defined by

$$\Gamma(E) = \frac{E+2E_0}{E+E_0}\,, \quad (6)$$

where E_0 is the rest mass energy per nucleon. Methods that find Φ from the current measurement of solar activity at the Sun, such as sunspot number, have been found to tend to precede the GCR modulation. The lag varies from 8 to 14 months and depends on solar magnetic field orientation. Thus, using sunspots has the advantage of predicting future GCR fluxes. However, using spacecraft instrument data such as ACE particle flux measurements more precisely emulates the actual GCR flux. The analysis shows that the correlation of the spectra of all the significant GCR elements (Z=1 to 28) is better using direct sampling of the heliosphere by spacecraft to find Φ, since direct measurement of the GCR flux by instrument samples the current state of the heliosphere. In the BON models, this is calculated from the best available data.

The Heliocentric Potential Modulation of the ISO LIS

The effect the interplanetary magnetic field on the GCR spectrum has been shown theoretically to be approximately equivalent to a Sun-centered electric potential with magnitude equal to the energy lost by the GCR particles in reaching Earth's orbit from outside the solar system (Gleeson and Axford, 1967). The effect of heliocentric potential on the primary GCR flux is described by equations 7 through 9:

$$F(E) = F_0(E_0) \cdot \left(\frac{P(E)}{P(E_0)}\right)^2, \quad (7)$$

$$E = E_0 - UZ, \quad (8)$$

$$P(E) = c^{-1}\sqrt{E^2 + 2AEmc^2}, \quad (9)$$

where m is the nucleon mass in MeV, c is the velocity of light in a vacuum, F_0 is the unmodulated flux having energy E_0, atomic weight A, and atomic number Z, P is the particle's momentum, E is the particle's energy after modulation, and U is the heliocentric potential in MV. New heliocentric potentials are calculated from the Apatity neutron monitor response to the incoming cosmic ray flux, though other sources could be used (O'Brien et al., 1996). The heliocentric potentials values are optimized to best reproduce historical data Deep River neutron monitor count rates and historic cosmic ray measurements when used with LUIN2000, the radiation transport model used by CARI-6 (O'Brien et al., 2003; Federal Aviation Administration [FAA], 2017). They continue to provide good results for dose rate at aviation altitudes when used with the cosmic ray shower data used by CARI-7 and -7A, and so they are retained to keep historical values of the heliocentric potential consistent from CARI-6 to CARI-7.

Solar Particle Events

Event-integrated proton spectra for several SPEs can be found in technical reports describing the Online Tool for the Assessment of Radiation in Space (Singleterry et al., 2010) and supporting references. Two of these are available for selection at runtime in CARI-7A: the Langley Research Center spectrum (Wilson et al., 1991) for the extreme SPE of Feb. 1956, and the Sauer et al. (1990) spectrum for the SPE of late Sept. 1989.

User-Defined Particle Spectra

Alternate models of the SPEs mentioned above and models of other SPEs, time-specific spectra from within SPEs, and alternate GCR spectral, can be used in CARI-7A calculations when called as user-defined spectra. A user-defined spectrum may be called by selecting spectrum #7 from runtime menus or indicating spectrum #7 in the appropriate input file. A user-defined spectrum is assumed to have units of particles/(cm^2 s sr GeV/n) and output is normalized as if the spectrum described GCR. When requested, the user-defined spectrum is read from folder GCR_MODELS, must be named MY_MODEL.OUT, and the spectrum file format (see Appendix B) should be identical to a BON11 GCR spectrum file (BO11_GCR.OUT). Thus, the format is two lines (maximum of 72 characters each) of text information and then 2800 lines of data in a three-column format: the first four spaces are read as an integer designating the atomic number, followed by two 11-character real numbers in engineering format for particle energy in GeV and flux, respectively.

CONCLUDING REMARKS

This report describes the cosmic radiation sources and modulation models available to users of CARI-7 and -7A for calculation of radiation spectra at Earth orbit before entering the magnetosphere. It in no way exhausts the subject of cosmic radiation and its effects. For example, exposure to ionizing radiation can result in serious health consequences, albeit at a very low level of risk at the expected exposure levels (Friedberg et al., 2002; Friedberg and Copeland, 2003; 2011; Copeland, 2013; Copeland and Friedberg, 2014; Wilson et al., 2005). Also, in addition to the biological concerns, cosmic radiation can cause soft errors in electronics in aircraft, can damage electronics on spacecraft (e.g., reducing the useful lifetime of components such as solar panels), and disable over-the-horizon radio communications (a *polar cap absorption* event: the solar radiation increases ionization and enhances absorption of radio signals passing through the region enough to absorb transpolar high-frequency radio transmissions) (Dyer et al., 2017).

Please see additional resources for a much broader discussion of cosmic radiation, space weather, and associated effects, for example, reports by Gaisser (2016) and Buzulukova (2018).

REFERENCES

Adams, J.H. Jr., Heiblim, S., Malott, C. (2009, July). *Evaluation of galactic cosmic ray models* [Paper presentation]. IEEE Nuclear Space and Radiation Effects Conference, Quebec City, QC, Canada. ntrs.nasa.gov/archive/nasa/casi.ntrs.nasa.gov/20090034942.pdf

Badhwar, G. D., & O'Neill, P. M. (1994). Long-term modulation of Galactic Cosmic Radiation and its model for space exploration. *Advances in Space Research: The Official Journal of the Committee on Space Research (COSPAR), 14*(10), 749–757. https://doi.org/10.1016/0273-1177(94)90537-1

Badhwar, G. D., & O'Neill, P. M. (1996). Galactic cosmic radiation model and its applications. *Advances in Space Research: The Official Journal of the Committee on Space Research (COSPAR), 17*(2), 7–17. https://doi.org/10.1016/0273-1177(95)00507-b.

Buzulukova, N. (Ed.). (2018). *Extreme Events in Geospace: Origins, Predictability and Consequences*. Elsevier.

Copeland, K. A. (2017). CARI-7A: Development and Validation. *Radiation Protection Dosimetry, 175*(4), 419-431. https://doi.org/10.1093/rpd/ncw369

Copeland, K., & Friedberg W. (2014). In-Flight Radiation Exposure. FAA Advisory Circular No. 120-61B. https://www.faa.gov/regulations_policies/ advisory_circulars/index.cfm/go/document.information/documentID/1026386

Copeland, K., & Atwell, W. (2019). Flight safety implications of the extreme solar proton event of 23 February 1956. *Advances in Space Research, 63*(1), 665-671. https://doi.org/10.1016/j.asr.2018.11.005.

Copeland, K. A., Sauer, H. H., Duke, F. E., & Friedberg, W. (2008). Cosmic radiation exposure of aircraft occupants on simulated high-latitude flights during solar proton events from 1 January 1986 through 1 January 2008. *Advances in Space Research: The Official Journal of the Committee on Space Research (COSPAR), 42*(6), 1008-1029.

Copeland, K. A. (2014). *Cosmic ray particle fluences in the atmosphere resulting from primary cosmic ray heavy ions and their resulting effects on dose rates to aircraft occupants as calculated with MCNPX 2.7.0.* Doctoral thesis, Royal Military College of Canada (RMCC). Massey Library Collection at RMCC and the Canadian National Archives in Ottawa, Canada.

Dyer, C., Hands, A., Ryden, K., & Lei, F. (2017). Extreme atmospheric radiation environments and single event effects. *IEEE Transactions on Nuclear Science, 65*(1), 432-438. https://doi.org/10.1109/TNS.2017.2761258

Ehmert, A. (1959). *On the Modulation of the Primary Spectrum of Cosmic Rays from Solar Activity.* Proceedings of the International Conference on Cosmic Rays 4, Moscow. 140.

Federal Aviation Administration. (2017). CARI-6: Radiobiology Research Team. https://www.faa.gov/data_research/research/med_humanfacs/aeromedical/radiobiology/cari6

Foelsche, T., Mendell, R. B., Wilson, J. W., & Adams, R. R. (1974). *Measured and Calculated Neutron Spectra and Dose Equivalent Rates at High Altitudes; Relevance to SST Operations and Space Research*. Report No. NASA TN D-7715. National Aeronautics and Space Administration.

Forbush, S. E. (1938). On cosmic-ray effects associated with magnetic storms. *Terrestrial Magnetism and Atmospheric Electricity, 43*(3), 203-218. https://doi.org/10.1029/TE043i003p00203

Friedberg, W., & Copeland, K. (2011). *Ionizing Radiation in Earth's Atmosphere and in Space Near Earth.* Report DOT/FAA/AM-11/9, Federal Aviation Administration Office of Aerospace Medicine. Retrieved January 24, 2019 from www.faa.gov/data_research/research/med_humanfacs/oamtechreports/2010s/media/201109.pdf

Friedberg, W., & Copeland, K. (2003). *What Aircrews Should Know About Their Occupational Exposure to Ionizing Radiation*. Federal Aviation Administration Office of Aerospace Medicine Report DOT/FAA/AM-03/16. www.faa.gov/data_research/research/med_humanfacs/oamtechreports/2000s/media/200316.pdf

Friedberg, W., Copeland, K., Duke, F. E., Nicholas, J. S., Darden, E. B., Jr, & O'Brien, K., 3rd (2002). Radiation exposure of aircrews. *Occupational Medicine: State of the Art Reviews (Philadelphia, Pa.), 17*(2), 293–v.

Gaisser, T. K., Engle, R., & Resconi, E. (2016). *Cosmic rays and particle physics, 2nd Ed.* Cambridge University Press.

Gleeson, L. J., & Axford, W. I. (1967). Cosmic rays in the interplanetary medium. *The Astrophysical Journal, 149*, L115.

Hörandel, J. R. (2013, February). *Early cosmic-ray work published in German*. In AIP Conference Proceedings (Vol. 1516, No. 1, pp. 52-60). American Institute of Physics.

International Standards Organization. (2004). *Space environment (natural and artificial) -- Galactic cosmic ray model. ISO TS 15930:2004.* www.iso.org/iso/home/store/catalogue_tc/catalogue_detail.htm?csnumber =37095&commid=46614

Lantos P. (2005). Forbush decrease effects on radiation dose received on-board aeroplanes. *Radiation Protection Dosimetry, 117*(4), 357–364. https://doi.org/10.1093/rpd/nci302

McDonald, F. B., Webber, W. R., & Reames, D. V. (2010). Unusual time histories of galactic and anomalous cosmic rays at 1 AU over the deep solar minimum of cycle 23/24. *Geophysical Research Letters, 37*(18). https://doi.org/10.1029/2010GL044218

Mertens, C. J., Meier, M. M., Brown, S., Norman, R. B., & Xu, X. (2013). NAIRAS aircraft radiation model development, dose climatology, and initial validation. *Space Weather: The International Journal of Research & Applications, 11*(10), 603–635. https://doi.org/10.1002/swe.20100

Nagoya University. (2015). World Data Center-Cosmic Rays. Data Coverage for Numerical Data (Long-format Files). http://cidas.isee.nagoya-u.ac.jp/WDCCR/datacoverage_num.html

National Aeronautics and Space Administration. (2012). Layers of the Sun. www.nasa.gov/mission_pages/iris/multimedia/layerzoo.html

National Oceanic and Atmospheric Administration. (n.d.). Solar proton events affecting the earth environment. https://umbra.nascom.nasa.gov/SEP/

National Oceanic and Atmospheric Administration. (n.d.) Space Weather Scales. https://www.swpc.noaa.gov/noaa-scales-explanation

Nobel Foundation. (1965). *Nobel lectures, including presentation speeches and laureates' biographies, physics 1922-1941*. Elsevier.

Nymmik, R. A., Panasyuk, M. I., Pervaja, T. I., & Suslov, A. A. (1992). A model of galactic cosmic ray fluxes. *International Journal of Radiation Applications and Instrumentation. Part D. Nuclear Tracks and Radiation Measurements, 20*(3), 427-429. https://doi.org/10.1016/1359-0189(92)90028-T

O'Brien, K. (1979). Secular variations in the production of cosmogenic isotopes in the Earth's atmosphere. *Journal of Geophysical Research: Space Physics, 84*(A2), 423-431. https://doi.org/10.1029/JA084iA02p00423

O'Brien, K., Friedberg, W., Sauer, H. H., & Smart, D. F. (1996). Atmospheric cosmic rays and solar energetic particles at aircraft altitudes. *Environment International, 22 Suppl 1*, S9–S44. https://doi.org/10.1016/s0160-4120(96)00086-4

O'Brien, K., Smart, D. F., Shea, M. A., Felsberger, E., Schrewe, U., Friedberg, W., & Copeland K. (2003). Worldwide radiation dosage calculations for air crew members. *Advances in Space Research: The Official Journal of the Committee on Space Research (COSPAR), 31*(4), 835–840.

Perricone, M. (2001). Balloon Flight Launches Cosmic Ray Education Project. https://www.fnal.gov/pub/ferminews/ferminews01-07-27/p3.html

Su, Y. J., Ma, L., Ergun, R. E., Pritchett, P. L., & Carlson, C. W. (2008). Short-burst auroral radiations in Alfvénic acceleration regions: FAST observations. *Journal of Geophysical Research: Space Physics, 113*(A8). https://doi.org/10.1029/2007JA012896

O'Neill P. M., & Foster C. C. (2013). *Badhwar-ONeill 2011 Galactic Cosmic Ray Flux Model Description.* Tech. Rep. NASA/TP-2013-217376.

O'Neill P. M., Gogle, S., & Slaba, T. C. (2015). *Badhwar-ONeill 2014 Galactic Cosmic Ray Flux Model Description.* Tech. Rep. NASA/TP-2015-218569.

O'Neill, P. M. (2010). Badhwar–O'Neill 2010 galactic cosmic ray flux model—Revised. *IEEE Transactions on Nuclear Science, 57*(6), 3148-3153. https://doi.org/10.1109/TNS.2010.2083688

Pierre Auger Collaboration, Abraham, J., Abreu, P., Aglietta, M., Aguirre, C., Allard, D., Allekotte, I., Allen, J., Allison, P., Alvarez, C., Alvarez-Muñiz, J., Ambrosio, M., Anchordoqui, L., Andringa, S., Anzalone, A., Aramo, C., Argirò, S., Arisaka, K., Armengaud, E., Arneodo, F., … Kégl, B. (2007). Correlation of the highest-energy cosmic rays with nearby extragalactic objects. *Science (New York, N.Y.), 318*(5852), 938–943. https://doi.org/10.1126/science.1151124

Polar Geophysical Institute. (n.d.) Neutron Monitors. http://pgia.ru/cosmicray/

Sunspot Index and Long-term Solar Observations. (n.d.) http://www.sidc.be/silso/

Sauer, H. H., Zwickl, R. D., & Ness, M. J. (1990). *Summary Data for the Solar Energetic Particle Events of August through December 1989*. Space Environment Laboratory, National Oceanic and Atmospheric Administration.

Singleterry, R. C., Jr., Blattnig, S. R., Clowdsley, M. S., Qualls, G. D., Sandridge, C. A., Simonsen, L. C., Norbury, J. W., Slaba, T. C., Walker, S. A., Badavi, F. F., Spangler, J. L., Au-mann, A. R., Zapp, E. N., Rutledge, R. D., Lee, K. T., & Norman, R. B. (2010). *OLTARIS: Online Tool for the Assessment of Radiation in Space.* NASA/TP–2010-216722. NASA Center for AeroSpace Information.

Smart, D. F., & Shea, M. A. (1997). Solar radiation. In: *Encyclopedia of Applied Physics 18* (pp. 393-429). VCH Publishers, Inc.

Wilson, J. G. (1976). *Cosmic Rays*. Springer-Verlag Inc.

Wilson, J. W., Mertens, C. J., Goldhagen, P., Friedberg, W., De Angelis, G., Clem, J. M., Copeland, K., & Bidasaria, H. B. (2005). *Atmospheric Ionizing Radiation and Human Exposure*. National Aeronautics and Space Administration Technical Publication NASA/TP-2005-213935. NASA Center for AeroSpace Information.

Wilson, J. W., Townsend, L. W., Schimmerling, W., Khandelwal, G. S., Khan, F., Nealy, J. E., Cucinotta, F. A., Simonsen, L. C., Shinn, J. L., & Norbury, J.W. (1991). *Transport Methods and Interactions for Space Radiations*. NASA Reference Publication 1257.

APPENDIX A: LAYERS OF THE SUN

Figure A1

Model of the Layers of the Sun

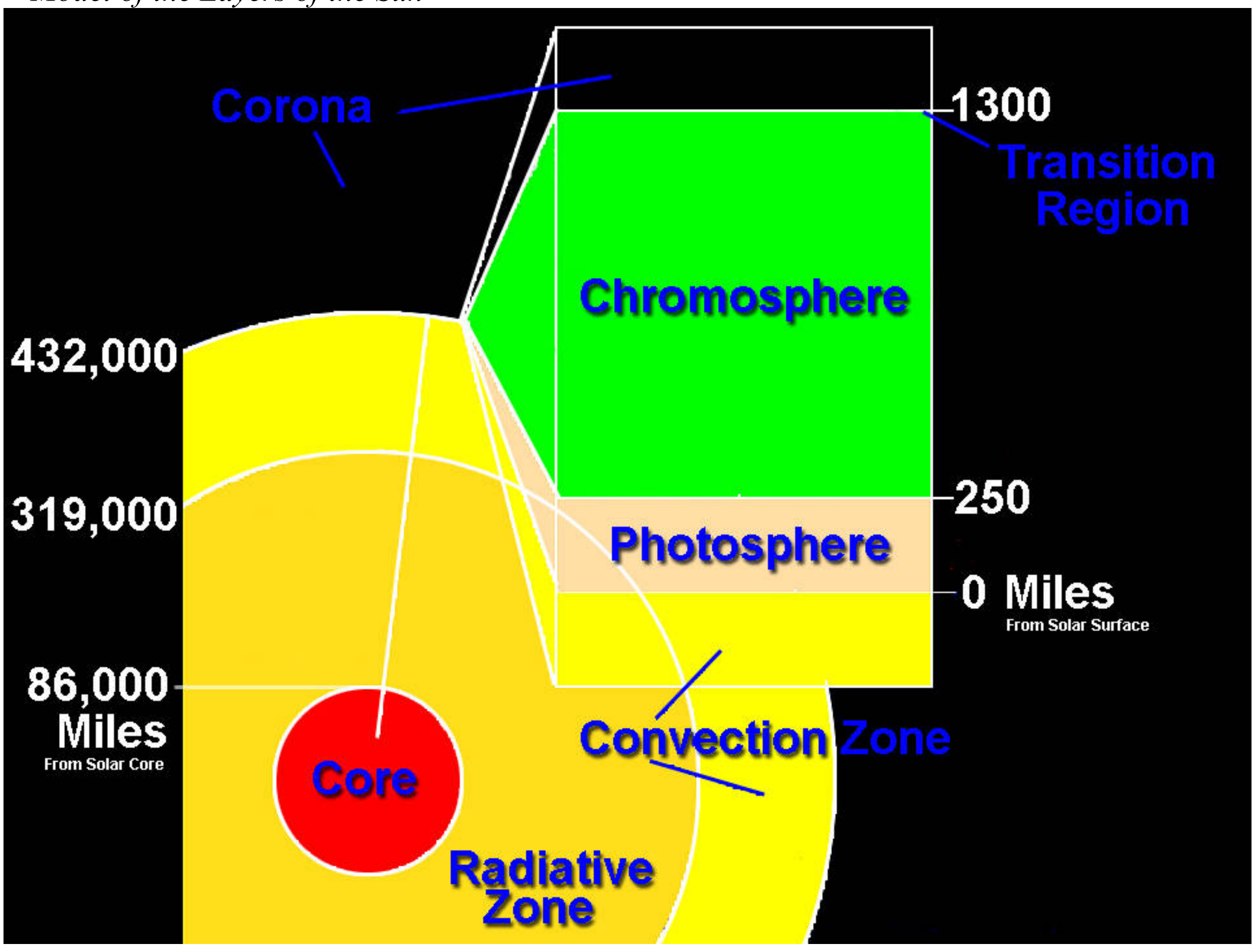

Note. For the inner layers, the mileage is from the Sun's core; for the outer layers, the mileage is from the Sun's surface. The inner layers are the Core, Radiative Zone, and Convection Zone. The outer layers are the Photosphere, the Chromosphere, the Transition Region, and the Corona. From "Layers of the Sun," by the National Aeronautics and Space Administration, 2012. (www.nasa.gov/mission_pages/iris/multimedia/layerzoo.html). In the public domain.

Photosphere - The photosphere is the deepest layer of the Sun that we can observe directly. It reaches from the surface visible at the solar disk center to about 250 miles (400 km) above that. The temperature in the photosphere varies between about 6500 K at the bottom and 4000 K at the top (11,000 °F/6200 °C to 6700 °F/3700 °C). Most of the photosphere is covered by granulation (National Aeronautics and Space Administration [NASA], 2012).

Chromosphere - The chromosphere is a layer in the Sun between about 250 miles (400 km) and 1300 miles (2100 km) above the solar surface (the photosphere). The temperature in the chromosphere varies between about 4000 K at the bottom (the so-called temperature minimum) and 8000 K at the top (6700 °F/3700 °C and 14,000°F/7700 °C). In this layer (and higher layers), temperatures rise as distance from the Sun increases, unlike in the lower layers where temperatures rise as distance from the center decreases (NASA, 2012).

Transition Region - The transition region is a very thin layer (60 miles / 100 km) between the chromosphere and the corona where the temperature rises abruptly from approximately 8000 K to 500,000 K (14,000 °F/7700 °C to 900,000 °F/ 500,000 °C) (NASA, 2012).

Corona - The corona is the Sun's outermost layer, starting at approximately 1300 miles (2100 km) above the solar surface (the photosphere). The corona's temperature is 500,000 K (900,000 °F, 500,000 °C) or more, up to a few million K. The corona is visible using a coronagraph or during a total solar eclipse. The corona does not have an upper limit (NASA, 2012).

APPENDIX B. USER-DEFINED SPECTRUM FILE FORMAT SAMPLE

A user-defined particle spectrum must be in the correct format to be read correctly. The first two lines of file MY_SPEC.OUT are assumed to be 72 characters or less of text. The remaining 2800 data lines are read from the file using a Fortran read with the predefined format of "I4,2ES11.3" which indicates an integer of four digits or fewer followed by two real numbers in engineering format as shown in the following edited sample (`courier new` font). The three columns are atomic charge, kinetic energy in units of GeV, and differential flux in units of particles/(cm^2 s sr GeV/n).

```
 1958.123      G11on20150118at0103.scr
  Z       E           F
   1  1.000E-02  1.085E+08
   1  1.150E-02  1.013E+08
   1  1.322E-02  9.459E+07
   .      .           .
   .      .           .
   .      .           .
   1  7.565E+03  6.668E-82
   1  8.697E+03  1.654E-82
   1  1.000E+04  4.095E-83
   2  4.000E-02  5.761E-37
   2  4.600E-02  2.664E-37
   2  5.288E-02  1.234E-37
   .      .           .
   .      .           .
   .      .           .
  28  4.463E+05  1.380E-86
  28  5.131E+05  3.423E-87
  28  5.900E+05  8.474E-88
```

When defining a spectrum, do not use 0.000E+00 to indicate a trivially small flux. Instead, as was done in the sample, use a very large negative exponent to indicate such a flux.